

# Tropical Climate Instability: The Last Glacial Cycle from a Qinghai-Tibetan Ice Core

L. G. Thompson,\* T. Yao, M. E. Davis, K. A. Henderson, E. Mosley-Thompson, P.-N. Lin, J. Beer, H.-A. Synal, J. Cole-Dai, J. F. Bolzan

An ice core record from the Guliya ice cap on the Qinghai-Tibetan Plateau provides evidence of regional climatic conditions over the last glacial cycle.  $^{36}\text{Cl}$  data suggest that the deepest 20 meters of the core may be more than 500,000 years old. The  $\delta^{18}\text{O}$  change across Termination I is  $\sim 5.4$  per mil, similar to that in the Huascarán (Peru) and polar ice cores. Three Guliya interstadials (Stages 3, 5a, and 5c) are marked by increases in  $\delta^{18}\text{O}$  values similar to that of the Holocene and Eemian ( $\sim 124,000$  years ago). The similarity of this pattern to that of  $\text{CH}_4$  records from polar ice cores indicates that global  $\text{CH}_4$  levels and the tropical hydrological cycle are linked. The Late Glacial Stage record contains numerous 200-year oscillations in  $\delta^{18}\text{O}$  values and in dust,  $\text{NH}_4^+$ , and  $\text{NO}_3^-$  levels.

The relative significance of 20th-century climatic and environmental changes must be assessed from the long-term global-scale perspective available from a spectrum of proxy histories, including those from ice cores. The Qinghai-Tibetan (Q-T) Plateau is one of the most imposing topographic features on Earth's surface, having a mean elevation of  $\sim 4.5$  km and an area of  $2.5 \times 10^6$  km $^2$ , one-third the size of the continental United States. The sensible heat flux and latent heat released over the Q-T Plateau drive the intense monsoon circulation and strongly influence global circulation patterns (1). Consequently, this region experiences a pronounced annual precipitation cycle and 70 to 80% of the total is during the summer monsoon (2).

Glaciers covering an area of  $\sim 46,600$  km $^2$  (3) are scattered across the Q-T Plateau. Ice core histories are particularly important because reliable meteorological observations and complementary paleoclimatic records are limited here. Cores drilled in 1987 on the Dundee ice cap (4) along the northeastern side of the Q-T Plateau (Fig. 1) provide a history of conditions during

both the Holocene and the latter part [back to  $\sim 40$  thousand years ago (ka)] of the glacial stage. On the Dundee ice cap, the pre-Holocene ice was confined to the bottom 10 m of the core and thus yielded little detailed information about the glacial stage. Here we present a subtropical ice core record from China that extends through the entire Holocene-Wisconsinan sequence.

In 1992 we recovered a 308.6 m core to bedrock from the Guliya ice cap (5) located at  $35^\circ 17' \text{N}$ ,  $81^\circ 29' \text{E}$  in the far western Kunlun Shan on the Qinghai-Tibetan Plateau, China (Fig. 1). The Guliya ice cap (summit elevation 6710 m above sea level) covers  $\sim 200$  km $^2$  and is part of an ice mass extending over 8000 km $^2$  in the western Kunlun Shan. The ice cap is surrounded by vertical ice walls 30 to 40 m high and has internal temperatures of  $-15.6^\circ\text{C}$  at 10 m,  $-5.9^\circ\text{C}$  at 200 m, and  $-2.1^\circ\text{C}$  at its base. Pit studies and accumulation stake measurements in 1990 and 1991 indicate that the ice cap receives  $\sim 200$  mm ( $\text{H}_2\text{O}$  equivalent) of accumulation per year.

**The Guliya core.** The core was recovered (Fig. 1) using an electromechanical drill in a dry hole to 200 m and a thermal drill with an alcohol-water mixture from 200 m to bedrock (308.6 m). No hiatus was observed in the core, and the visible layers were horizontal throughout. The entire length of the frozen core was analyzed by cutting 12,628 samples for oxygen isotopic ( $\delta^{18}\text{O}$ ) measurements, 12,480 samples for dust concentrations, and 9681 samples for anion  $\text{Cl}^-$ ,  $\text{NO}_3^-$ , and  $\text{SO}_4^{2-}$  concentrations.

$\delta^{18}\text{O}$  values are a proxy for past atmospheric temperature over northern Tibet

(6), and the Guliya  $\delta^{18}\text{O}$  record shows five intervals of low (more negative)  $\delta^{18}\text{O}$  values between 150 and 265 m (Fig. 2). Ice in the lowest 40 m has high (less negative)  $\delta^{18}\text{O}$  values. Between 150 and 260 m, the average concentration of dust (diameters of 0.63 to 50.0  $\mu\text{m}$ ) is 6% higher than in the ice above this interval and 37% higher than concentrations in the ice immediately below it. From 180 to 260 m, the ice with lower  $\delta^{18}\text{O}$  values also has high dust concentrations, and below 290 m the dust content increases 100-fold. The highest concentrations are just above the bedrock contact, where a number of small pebbles in the lowest 10 cm represent basal material.

Two of the anions ( $\text{Cl}^-$  and  $\text{SO}_4^{2-}$ ) originate primarily from surface dust, including dust from salt flats and lake beds that dot the western side of the plateau. The current average  $\text{Cl}^-$  and  $\text{SO}_4^{2-}$  concentrations on the Guliya ice cap are  $\sim 50\%$  and 23% lower, respectively, than those on the Dundee ice cap, which is nestled among several major deserts on the northeast side of the plateau (4). The probable precursors of  $\text{NO}_3^-$  in the snowfall are tropospheric nitrogen species (for example,  $\text{NH}_4^+$  and  $\text{NO}_x$ ) originating from sources such as soils, vegetation, and lightning (7). As with the high dust concentrations, high concentrations of  $\text{Cl}^-$  and  $\text{SO}_4^{2-}$  are associated with low  $\delta^{18}\text{O}$  values between 180 and 250 m. In the lowest 18 m of the core, the concentrations of  $\text{Cl}^-$ ,  $\text{SO}_4^{2-}$  and  $\text{NO}_3^-$  decline sharply, whereas dust concentrations increase by two orders of magnitude. These different aerosol patterns suggest that environmental changes affected their respective source areas differently then.

**Time-scale development.** Interpretation of the paleoclimatic information within the Guliya core requires development of a time scale. Most of the ice core history (for example, strata older than 2 ka) is preserved below 120 m, where substantial thinning precludes counting layers. We used the apparent correlation between atmospheric  $\text{CH}_4$  levels and stadial and interstadial events inferred from  $\delta^{18}\text{O}$  values in polar

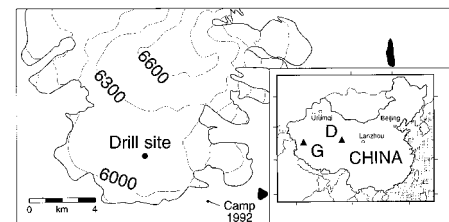


**Fig. 1.** The locations of the Guliya (G) and Dundee (D) ice caps and the site where the 308.6-m Guliya core was drilled. Drill site elevation, 6200 m above sea level.

L. G. Thompson, M. E. Davis, K. A. Henderson, and J. F. Bolzan are at the Byrd Polar Research Center and Department of Geological Sciences, Ohio State University, Columbus, OH 43210, USA. T. Yao is at the Lanzhou Institute of Glaciology and Geocryology, Lanzhou, China. E. Mosley-Thompson is at the Byrd Polar Research Center and Department of Geography, Ohio State University, Columbus, OH 43210, USA. P.-N. Lin and J. Cole-Dai are at the Byrd Polar Research Center, Ohio State University, Columbus, OH 43210, USA. J. Beer is at the Swiss Federal Institute for Environmental Science and Technology, Dübendorf, Switzerland. H.-A. Synal is at the Paul Scherrer Institute, Zurich, Switzerland.

\*To whom correspondence should be addressed. E-mail: thompson.3@osu.edu.

cores (Fig. 3) to establish the Guliya time scale for the past 110,000 years. The linkage between the polar records and the Guliya record is reasonable because low-latitude moisture and temperature fluctuations likely have driven global atmospheric CH<sub>4</sub> concentrations (8), particularly during the LGS (Late Glacial Stage), when the high north-

ern latitudes were covered with ice and the extent of vegetation was restricted (9).

We thus could match (10) the top 266 m (110 ka) of the Guliya δ<sup>18</sup>O record (Fig. 3B) with the GISP2 CH<sub>4</sub> record (Fig. 3A). The characteristic magnitudes and shapes of most of the interstadial peaks and stadial valleys of the GISP2 CH<sub>4</sub> record are repro-

duced in the Guliya δ<sup>18</sup>O record. Changes in global atmospheric CH<sub>4</sub> concentrations (11) reflect the balance of the primary sources (terrestrial emissions driven by changes in temperature and precipitation) versus the efficiency of the primary sink (oxidation by OH<sup>-</sup>). Ice older than 110 ka in the GISP2 and GRIP cores is folded (12). Thus, below 266 m (Fig. 3B, light blue) we assigned a single tie point between the Guliya δ<sup>18</sup>O and the Vostok δD records (Fig. 3C). The Guliya δ<sup>18</sup>O pattern appears similar to the Vostok Eemian CO<sub>2</sub> record (13) (Fig. 3C). Stage 6 ice is not clearly indicated in the Guliya δ<sup>18</sup>O record; thus, construction of a time scale in this manner before 132 ka is precluded. Figure 3, A and C, illustrate the polar CH<sub>4</sub> (11) and stable isotope records (14, 15) on a time scale (16) that correlates the Vostok record with the SPECMAP record (17). Thus, the Guliya δ<sup>18</sup>O record is linked by extrapolation to the SPECMAP chronology, under the assumption that the methane fluctuations in high-latitude ice cores are synchronous with stable isotope variations in western China.

Our proposed time scale requires that annual layers have thinned rapidly with depth in the upper part of the ice cap. This type of flow is different from that in polar ice sheets, where vertical strain rate in the upper half is nearly constant, but it is similar to deformation in the Dunde ice cap (4). Measured annual layer thicknesses in the upper 75% of the Dunde core indicate that vertical strain rate in the upper half of the ice cap decreases rapidly. For the nearly two-dimensional flow around the borehole on Guliya, measured surface velocities show a surface vertical strain rate that is two to three times the average longitudinal strain rate, consistent with the vertical strain rate profile on Dunde. This anomalous flow is supported by (i) the temperature profile, which is more linear with depth than expected if horizontal advection is important, and (ii) the ice crystal orientations, which lack the tightly clustered vertical *c*-axis orientation with depth that is expected when deformation is dominated by simple shear. These orientations suggest that the shear stress does not increase as rapidly with depth as predicted by a laminar flow model, and that longitudinal stresses dominate the effective shear stress throughout most of the ice depth.

To further test our time scale, we assumed that the vertical strain rate has the Class I form discussed by Thompson *et al.* (18), and then we derived an accumulation rate history consistent with the Guliya time scale. The vertical velocity was computed as a function of depth, and the accumulation rate was adjusted between 18 primary

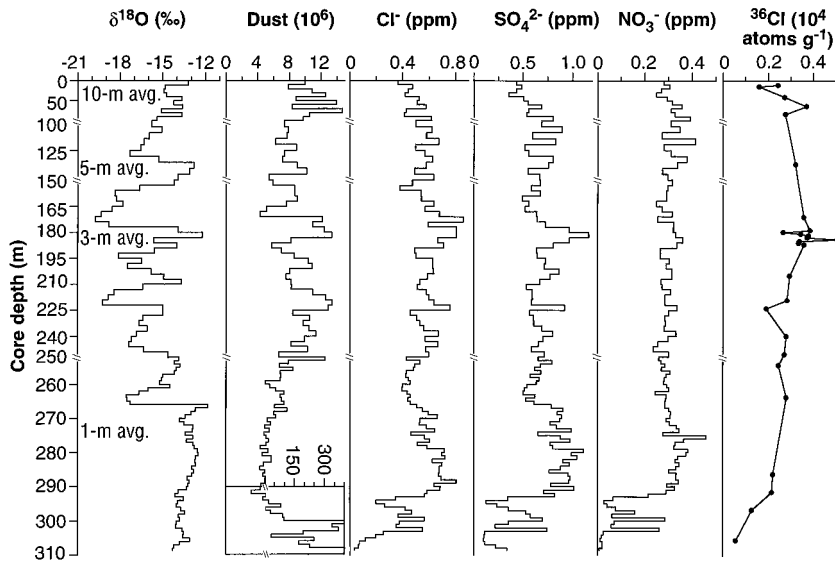


**Fig. 2.** Depth along the Guliya core and the averages of (from left to right) δ<sup>18</sup>O values, the concentrations of dust, Cl<sup>-</sup>, SO<sub>4</sub><sup>2-</sup>, NO<sub>3</sub><sup>-</sup>, and <sup>36</sup>Cl. Except for the <sup>36</sup>Cl concentrations, the parameters are averaged for decreasing depth intervals down the core to account for layer thinning. Dust reflects the number of particles (0.63 to 50 μm diameter) per milliliter sample. In the inset at bottom, the dust concentration at 300 to 301 m depth is 8.53 × 10<sup>8</sup>; at 308 m, it is 1.52 × 10<sup>13</sup>.

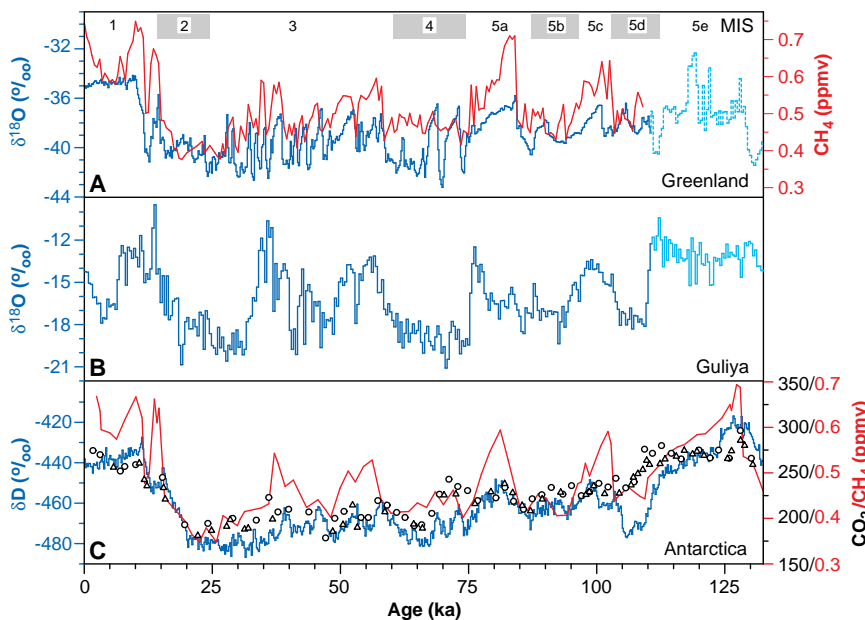


**Fig. 3.** (A) The GISP2 δ<sup>18</sup>O (blue) and CH<sub>4</sub> records (red) are shown with time for the past 132 ka (11). The record is compromised by ice deformation below 110 ka, as shown by the light blue dotted line. The Guliya δ<sup>18</sup>O record over the past 110 ka (B) is matched to the GISP2 CH<sub>4</sub> record over the past 110 ka. The Guliya record is also compared to the Vostok δD (blue), CH<sub>4</sub> (red) and CO<sub>2</sub> (black) [(13); circles, 1987 data; triangles, 1991 data] records (C), which display temporal continuity below isotope Stage 5d.

match points until the calculated ages agreed with the transferred time scale. The inferred accumulation rate during the early and mid-glacial was similar to the current value but dropped to  $\sim 40 \text{ mm a}^{-1}$  between 35 and 7 ka. These values are not unreasonable, and suggest that the mid- to late glacial stage climate was much drier than at present, in which the decrease in accumulation rate was similar to that observed in polar ice cores (19).

**Evidence for old ice (>500 ka).** Ice older than 100 ka can be dated using  $^{36}\text{Cl}$ , which has a half-life of  $3.01 \times 10^5$  years (20). Analysis of 27 samples showed that the  $^{36}\text{Cl}$  activity decreases from the surface to the bottom of the Guliya core (Fig. 2). The age of the near-bottom ice, below the applicability of the  $\text{CH}_4$ - $\delta^{18}\text{O}$  dating, can be estimated by substituting the activities of

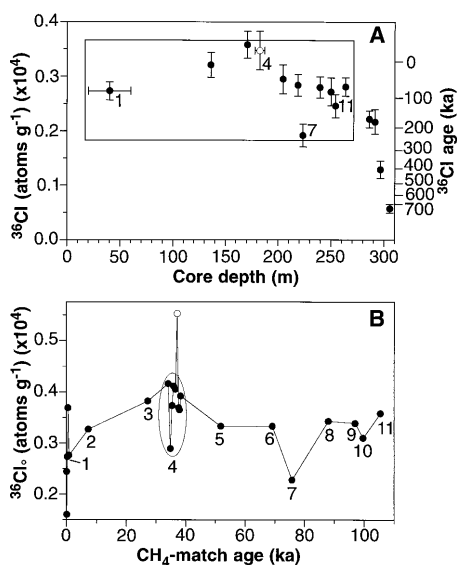


**Fig. 4.** (A)  $^{36}\text{Cl}$  measurements [atoms ( $\times 10^4$ ) per gram of ice] for 15 Guliya ice core samples are plotted with depth. The upper 11 samples, with ages younger than 110 ka, are assumed to represent modern concentrations. Note that the value of sample 4, denoted by (○), is the average of eight of the nine consecutive samples shown in (B). The error bars indicate the instrumental errors, except for the averaged value (4) for which the error bar indicates the  $1\sigma$  range of the eight individual measurements. Of the five samples from the upper 100 m of the core (Fig. 2), only sample 1 was used in the calculation of the modern concentration because it encompasses the greatest amount of time (depth interval: 20 to 60 m). The depth-versus-age relation (as described in the text) is shown on the right axis and is applicable only for the bottom four samples. The bottom two samples have low  $^{36}\text{Cl}$  concentrations, and the estimated age for the bottom sample is  $\sim 760$  ka. (B) The calculated  $^{36}\text{Cl}$  values for each of the 11 sets of ice core samples are shown with time. The  $^{36}\text{Cl}$  values for the eight samples in set 4 are shown along with the high value denoted by (○) at 40 ka (183 m).

the bottom four samples into the radioactivity decay equation. The initial activity ( $^{36}\text{Cl}_0$ ) is assumed to be equal to the modern (pre-nuclear testing) activity and the decay constant ( $\lambda$ ) is  $2.30 \times 10^{-6} \text{ a}^{-1}$ . The modern activity was estimated as the average of the  $^{36}\text{Cl}_0$  values for the 11 sections of core shown in the box in Fig. 4A. Each sample's  $^{36}\text{Cl}_0$  was calculated by substituting the measured value of  $^{36}\text{Cl}$  and the estimated age into the decay equation. The average  $^{36}\text{Cl}_0$  for the past  $\sim 100,000$  years is  $0.328 \times 10^4$  atoms per gram (Fig. 4B). The result (Fig. 4A) illustrates that the ice below a depth of 290 m in the ice is  $^{36}\text{Cl}$ -dead, indicating that the ice is  $>500,000$  years old, although true ages cannot be determined. In this simple calculation, we assumed that the production rate was unchanged before 100 ka.

Cosmogenic radioisotopes can also be used to synchronize ice cores and sedimentary archives (21, 22). We measured  $^{36}\text{Cl}$  activities for a section of core from 178 to 187 m (Fig. 2; also point 4 in Fig. 4A). The section was cut into a continuous sequence of nine samples representing ice deposited around 35 to 40 ka according to our time scale (Figs. 3 and 4B). The  $^{36}\text{Cl}$  concentration in one sample of that sequence is roughly twice the average concentration for all other samples younger than 110 ka. Within the uncertainties of the ice core time scales, this  $^{36}\text{Cl}$  event may be correlative with a high  $^{10}\text{Be}$  and  $^{36}\text{Cl}$  event recorded in the Antarctic cores from Vostok and Dome C (21) and from Byrd Station (23) around 40 ka. A similar event is present in sediment cores from the Gulf of California (24) and Mediterranean Sea (22). The presence of this  $^{36}\text{Cl}$  marker in the predicted section of core lends support for the time scale we developed. The  $^{36}\text{Cl}$  spike occurs in a single sample representing about a 500-year period.

**The last glacial–interglacial cycle.** The last glacial stage (Wisconsinan/Würm) part of the Guliya record ( $\sim 10$  to 110 ka) is punctuated by a sequence of stadial and interstadial events (Fig. 3B), similar to

those in the GISP2 (14), GRIP (25), and Vostok (15) cores and in the SPECMAP (16) record. Unlike the polar  $\delta^{18}\text{O}$  records (Fig. 3, A and C), the Guliya  $\delta^{18}\text{O}$  values and the polar  $\text{CH}_4$  concentrations are comparable between the interglacials and interstadials. These variations suggest that atmospheric  $\text{CH}_4$  concentrations were affected primarily by variations in the vigor of the tropical hydrological cycle (8) rather than by processes in the polar regions. The  $\delta^{18}\text{O}$  values of the interstadials in Guliya also imply that subtropical climate was forced more strongly by precession (23 ka) than by obliquity (41 ka) (evident in the more negative  $\delta^{18}\text{O}$  values of ice representing Stages 2, 4, and 5d). Precessional dominance is expected in the mid-latitudes of the Northern Hemisphere either directly from solar forcing (caloric summer insolation) or from a moisture feedback amplification of the 23-ka cycle (26).

$\delta^{18}\text{O}$  values decrease during the major stadials, and the lowest values are at the Late Glacial Maximum (LGM), consistent with the  $\delta^{18}\text{O}$  patterns in polar records. The  $\delta^{18}\text{O}$  increase of 5.4‰ from the LGM to the Holocene is also similar to that in polar cores (14, 15) and in the Huascarán core (27) (Table 1). These data contribute to the growing body of evidence (28, 29) that the tropical climate was cool and variable during the last glacial cycle. Because the precipitation regime on Guliya is monsoonal, a strong link is expected between the tropical hydrological cycle and the atmospheric dynamics over the Q-T Plateau.

**Abrupt climate changes in the LGS.** Between 15 and 33 ka, the ice core record contains approximately 100  $\delta^{18}\text{O}$  oscillations with amplitudes from  $\sim 2$  to 21‰ and an average period of 200 years (Fig. 5A). The Greenland ice core  $\delta^{18}\text{O}$  record (25) also reveals abrupt warm events, called Dansgaard-Oeschger (D-O) events, during Stage 2. These are postulated to reflect large changes in the temperature and atmospheric circulation around Greenland on centennial to millennial time scales and have been attributed to abrupt changes in

**Table 1.**  $\delta^{18}\text{O}$  values (‰) for Guliya, Huascarán (27) and GISP2 (14, 36), along with  $\delta\text{D}$  values for Vostok (15), averaged over the 3200 years following and preceding the deglaciation sequence ( $\sim 10$  to 18 ka). The 200- and 400-year averages shown in Fig. 3 were used in the calculations. Note that averages for two time intervals (LGM: 18–21.2 ka and 21.0–24.2 ka) are shown for the Vostok core to account for the  $\sim 3000$ -year lead time (43), and the  $\delta^{18}\text{O}$  equivalents ( $\delta\text{D} = 8\delta^{18}\text{O} + 10$ ) are shown in parentheses.

Core	Early Holocene (6.8 to 10.0 ka)	LGM (18.0 to 21.2 ka)	Difference
Guliya (west China)	–13.1	–18.5	5.4
Huascarán (Peru)	–16.6	–22.9	6.3
GISP2 (Greenland)	–34.6	–39.7	5.1
Vostok (Antarctica)	–435.9 (–55.7)	–471.8 (–60.2)	36.0 (4.5)
Vostok (21.0 to 24.2 ka)		–479.2 (–61.1)	43.3 (5.4)

the thermohaline circulation in the Atlantic Ocean (29). In the Greenland cores, the D-O events, lasting several millennia, coincide with reduced levels of dust and high  $\delta^{18}\text{O}$  values and thus are quite different from the Guliya  $\delta^{18}\text{O}$  oscillations. Short-term ( $\sim 200$ -year) cycles have also been found in records from marine cores from the west side of the Antarctic Peninsula (30). One possible forcing mechanism is solar variability because there is evidence of a 200-year cycle in sunspot activity (31, 32).

Many of the peaks are marked by high concentrations of ammonium ( $\text{NH}_4^+$ ), and  $\text{NO}_3^-$  (Fig. 5, D and E) and are preceded slightly by an increase in the percentage of coarse (diameters  $>1.0 \mu\text{m}$ ) dust (Fig. 5, B and C). Increases in  $\text{NH}_4^+$  concentrations in the GRIP core are attributed to reductions in North American ice cover (33), because vegetation and other biological activity are major natural sources. Similarly,  $\text{NH}_4^+$  concentrations, and to a lesser degree  $\text{NO}_3^-$  concentrations, from the Guliya core may reflect the extent of deglaciated area on the Q-T Plateau or Eurasia.

The mechanisms causing these abrupt, oscillatory changes in environmental conditions are not clear. Variations in climate over Asia and the strength of the southeast Asian monsoon may be linked to the disappearance of high-elevation snow fields (34, 35). Reduced snow cover would lower the albedo, whereas the exposed soils would increase the radiative heating of the surface. Thus, glacial stage conditions may have been punctuated by brief, decade-long to century-long periods of reduced snow cover. We postulate that warmer conditions reduce snow cover on the plateau; as a result, dust is more easily entrained into the atmosphere. When mild conditions are sustained, increased biological activity would increase atmospheric  $\text{NH}_4^+$  and  $\text{NO}_3^-$  concentrations. The large  $\delta^{18}\text{O}$  oscillations (up to 22‰) cannot be accounted for solely by temperature variations. A likely mechanism may involve changes in the position of the semipermanent high-pressure system over the Q-T Plateau in response to an altered surface thermal regime.

**Deglaciation sequence.** The termina-

tion of the LGS is at  $\sim 150$  m in the Guliya core (Fig. 6A), where  $\delta^{18}\text{O}$  values rise in steps from a minimum at 158 m toward a reversal event between 146.5 and 149.5 m, which we interpret as the Younger Dryas (YD). Subsequently,  $\delta^{18}\text{O}$  values rise to early Holocene (Preboreal) values of  $-13\text{‰}$ . The Guliya  $\delta^{18}\text{O}$  record contrasts with that from Greenland (Fig. 6B), which shows an abrupt rise followed by a decrease (cooling) from the early Bølling ( $\sim 15$  ka) to the YD (36, 37). The overall geometry of the  $\sim 5.4\text{‰}$   $\delta^{18}\text{O}$  rise on Guliya more closely resembles the deglaciation record from the Huascarán, Peru, ice core (27). This similarity (Fig. 6, A and C) suggests that the climatic link between the Guliya and Huascarán regions during Termination I is stronger than that between Guliya and Greenland.

Without a precise dating tool, we cannot exactly correlate  $\delta^{18}\text{O}$  features between the Guliya and Huascarán cores. Time scales for both cores have been determined by matching them to appropriate well-dated records. The Huascarán core (27) (Fig. 6C) was

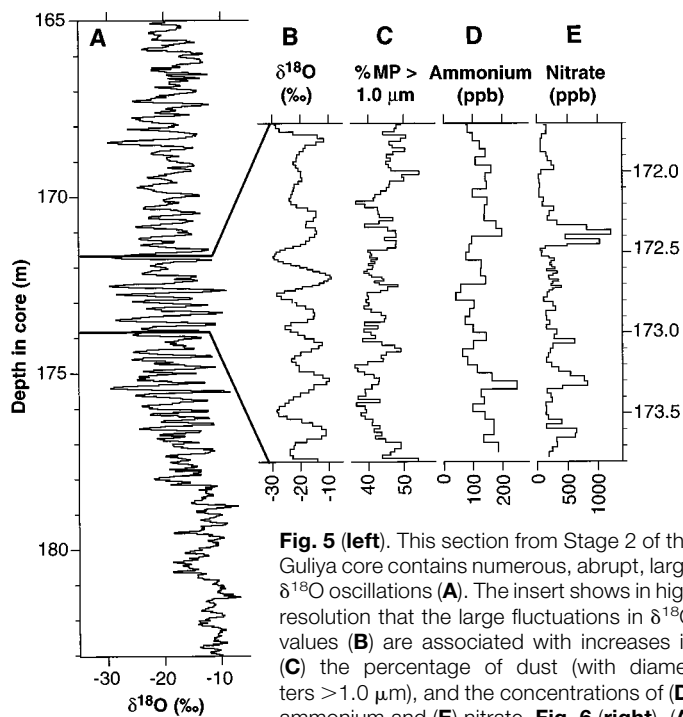
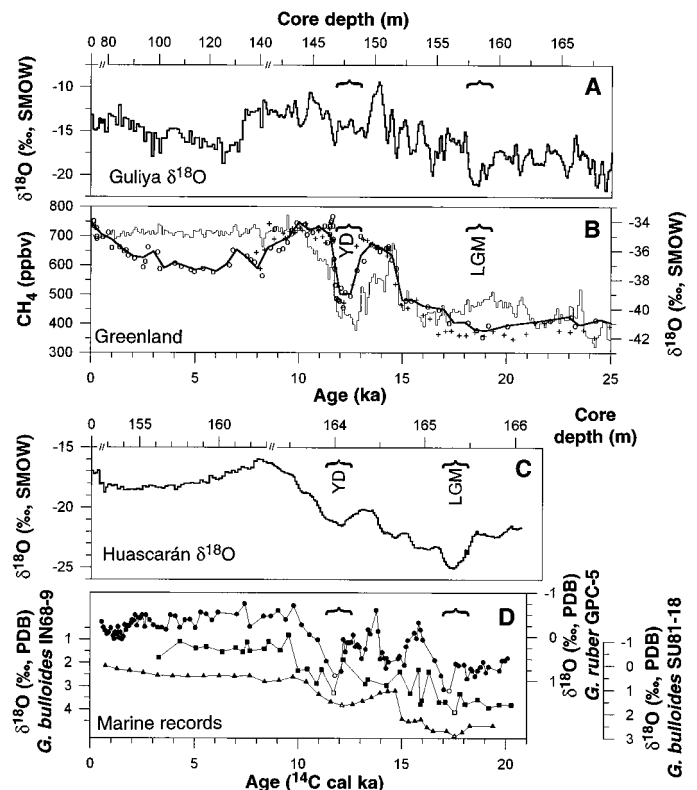


**Fig. 5 (left).** This section from Stage 2 of the Guliya core contains numerous, abrupt, large  $\delta^{18}\text{O}$  oscillations (A). The insert shows in high resolution that the large fluctuations in  $\delta^{18}\text{O}$  values (B) are associated with increases in (C) the percentage of dust (with diameters  $>1.0 \mu\text{m}$ ), and the concentrations of (D) ammonium and (E) nitrate. **Fig. 6 (right).** (A) The Guliya  $\delta^{18}\text{O}$  record covering the last deglaciation on a depth scale is compared with the (B) Greenland  $\text{CH}_4$  (GRIP, +; GISP2,  $\circ$ ) and  $\delta^{18}\text{O}$  profiles (GISP2, thin line). 500-year averages of GISP2  $\text{CH}_4$  are also shown (thick line). The deglaciation sequence (C) from Huascarán  $\delta^{18}\text{O}$  is compared to (D) several Northern Hemisphere marine records as additional confirmation of the timing of the deglaciation sequence in the Guliya core. Marine records include (top to bottom) (i) core KNR31 GPC-5 (47) from the Bermuda rise (4583 m) which is heavily  $^{14}\text{C}$ -dated and displays the YD event and an earlier maximum at 17.0 to 17.3  $^{14}\text{C}$  (open symbols); (ii) core IN68-9 (48) in the southern Adriatic Sea (1234 m), a site in closer geographical proximity to Guliya; and (iii) core SU81-18 (38) from the Atlantic Ocean west of Portugal (3135 m).



The time scales shown for the Bermuda Rise and Adriatic Sea cores were established from the published  $^{14}\text{C}$  dates using the same calibration method as for SU81-18 (40), except that linear interpolation was used between individual  $^{14}\text{C}$  dates. The Guliya and Huascarán  $\delta^{18}\text{O}$  records are averaged over successively smaller depth intervals 10, 1 and 0.1 m and 20, 0.2 and 0.02 m respectively. The averaging intervals are indicated by breaks in the depth at 80 m and 141 m in Guliya and at 153 m and 163.3 m in Huascarán. Below 140 m, the 0.1-m averages of Guliya  $\delta^{18}\text{O}$  are smoothed using a 5-point (1,3,4,3,1) filter, whereas all other  $\delta^{18}\text{O}$  averages shown are unsmoothed.

originally correlated with the  $\delta^{18}\text{O}$  (*G. bulloides*) profile in ocean core SU81-18 (38–40). This correlation has been supported by subsequent studies (41), and the ice core record is also similar to  $\delta^{18}\text{O}$  records from marine cores (42) from other nonpolar Northern Hemisphere sites (Fig. 6D). The date of the  $\text{CH}_4$  minimum in the GISP2 core is 18.9 ka, and the  $\delta^{18}\text{O}$  maximum for the SU81-18 core is at 17.5 ka (calibrated  $^{14}\text{C}$  age). Thus, we suggest that the timing of the LGM in the tropics and subtropics may lie between these dates (43) and that the age for the LGM  $\delta^{18}\text{O}$  minima in Guliya (158 m) and Huascarán (165.3 m) is  $18 \pm 1$  ka. Furthermore, the uncertainties in the radiocarbon calibration of the ocean cores and in visible layer counting in Greenland cores may allow the LGM to be coeval in all these records.

Although the magnitude of the  $\delta^{18}\text{O}$  deglaciation shift is comparable with that of other polar and equatorial ice core records, the onset in lower latitudes appears to predate the warming in central Greenland by several thousand years. A similar early warming in records from Antarctica and the Southern Ocean leads the warming in Greenland by 3300 years (43).

**The Holocene.** The relationship between high  $\delta^{18}\text{O}$  values in the Guliya core and high atmospheric  $\text{CH}_4$  levels continues throughout the Holocene as well. In the early Holocene, both  $\text{CH}_4$  concentrations and  $\delta^{18}\text{O}$  values are high (Fig. 3), whereas in the mid-Holocene both decrease. In the past 5000 years, both increase again. An early Holocene increase in  $\delta^{18}\text{O}$  values in the Guliya and Huascarán cores (27) is also consistent.

Paleoclimate data, including African lake levels, pollen, archaeological evidence, and a climate model study (44), suggest that the tropics were moister during the early to middle Holocene (6 to 9 ka) in response to intensification of the monsoon. A coeval intensification of the monsoon over Asia is inferred primarily from lake levels and lake sediments, which indicate that the climate of central and northern China was warmer and wetter in the early to mid-Holocene (45, 46). The Guliya  $\delta^{18}\text{O}$  record suggests that higher levels of atmospheric  $\text{CH}_4$  in the early Holocene are correlative with warmer, moister conditions in the subtropics and argues strongly for a low-latitude methane source at that time.

## REFERENCES AND NOTES

- P. J. Webster, in *Monsoons*, J. Fein, Ed. (Wiley, New York, 1987), pp. 3–32.
- PAGES, Series 93-1, R. Bradley, Ed. (IGBP-PAGES, Berne, Switzerland, 1993).
- Z. Wang and H. Yang, *Ann. Glaciol.* **16**, 17 (1992).
- L. G. Thompson *et al.*, *Science* **246**, 474 (1989).
- L. G. Thompson *et al.*, *Ann. Glaciol.* **21**, 175 (1995).
- T. Yao *et al.*, *J. Geophys. Res.* **101**, 29,531 (1996).
- J. A. Logan, *ibid.* **88**, 10,785 (1983); E. W. Wolff, *NATO-ASI Ser.* **30**, 195 (1995).
- N. Petit-Maire, M. Fontugne, C. Rouland, *Palaeogeogr. Palaeoclimatol. Palaeoecol.* **86**, 197 (1991); F. A. Street-Perrott, *Nature* **355**, 23 (1992); E. Bard, F. Rostek, C. Sonzogni, *ibid.* **385**, 707 (1997).
- J. Chappellaz *et al.*, *Nature* **366**, 443 (1993).
- The time scale transfer [D. Paillard, L. Labeyrie, P. Yiou, *Eos* **77**, 379 (1996)] involved 42 intermediate depth-to-age match points based on the most prominent features of each record. The selected features were spaced relatively evenly in time and a linear fit, assuming constant layer thickness, was used between successive points.
- E. J. Brook, T. Sowers, J. Orcharto, *Science* **273**, 1087 (1996).
- R. B. Alley *et al.*, *Nature* **373**, 394 (1995).
- J. M. Barnola, D. Raynaud, Y. S. Korotkevich, C. Lorius, *ibid.* **329**, 408 (1987); J. M. Barnola, P. Pimienta, D. Raynaud, Y. S. Korotkevich, *Tellus* **43B**, 83 (1991).
- P. M. Grootes, M. Stuiver, J. W. C. White, S. Johnsen, J. Jouzel, *Nature* **366**, 552 (1993).
- J. Jouzel *et al.*, *ibid.* **329**, 403 (1987).
- T. Sowers *et al.*, *Paleoceanography* **8** (no. 6), 736 (1993).
- The time scale for the upper 50 ka of GISP2 is based on visible layer counting and derived by correlation of the respective  $\delta^{18}\text{O}$  records of atmospheric  $\text{O}_2$  ( $\delta^{18}\text{O}_{\text{atm}}$ ) to transfer the Vostok chronology to GISP2 only below 50 ka. Hence, the two methane records are tied to the SPECMAP chronology, within the reported errors of the cross-hemispheric matching of  $\delta^{18}\text{O}_{\text{atm}}$  and the match between Vostok  $\delta^{18}\text{O}_{\text{atm}}$  and the  $\delta^{18}\text{O}$  in core V19-30 from the eastern tropical Pacific (16).
- L. G. Thompson *et al.*, *J. Glaciol.* **28** (no. 98), 57 (1982).
- R. B. Alley *et al.*, *Nature* **362**, 527 (1993).
- H. W. Bentley, F. M. Phillips, S. N. Davis, *Handbook Environment. Isotope Geochem.*, **2**, 427 (1986).
- G. M. Raisbeck *et al.*, *Nature* **326**, 273 (1987).
- G. C. Castagnoli *et al.*, *Geophys. Res. Lett.* **22** (no. 6), 707 (1995).
- J. Beer *et al.*, *NATO ASI Ser.* **12**, 141 (1992).
- L. McHargue, P. Damon, D. Donahue, *Proc. 23rd Int. Cosmic Ray Conf.* **3**, 854 (1993).
- S. J. Johnsen *et al.*, *Nature* **359**, 311 (1992).
- A. L. Berger, *Quat. Res.* **9**, 139 (1978); W. F. Ruddiman and A. McIntyre, *Geol. Soc. Am. Bull.* **95**, 381 (1984).
- L. G. Thompson *et al.*, *Science* **269**, 46 (1995).
- T. P. Guilderson, R. G. Fairbanks, J. L. Rubenstein, *ibid.* **263**, 663 (1994); M. Stute *et al.*, *ibid.* **269**, 379 (1995); R. S. Webb, D. H. Rind, S. J. Lehman, R. J. Healy, D. Sigman, *Nature* **385**, 695 (1997); P. A. Colinvaux, P. E. De Oliveira, J. E. Moreno, M. C. Miller, M. B. Bush, *Science* **274**, 85 (1996).
- W. S. Broecker, *Oceanography* **4**, 79 (1991).
- A. Leventer *et al.*, *Geol. Soc. Am. Bull.* **108** (no. 12), 1626 (1996).
- M. Stuiver and T. F. Braziunas, *Nature* **338**, 405 (1989).
- H. E. Suess and T. W. Linick, *Philos. Trans. R. Soc. London Ser. A* **330**, 403 (1990); M. Stuiver and T. F. Braziunas, *Holocene* **3**, 289 (1993).
- K. Fuhrer, A. Neftel, M. Anklin, T. Staffelbach, M. Legrand, *J. Geophys. Res.* **101** (no. D2), 4147 (1996).
- F. M. Sirocko *et al.*, *Nature* **364**, 322 (1993).
- T. P. Barnett, L. Dumenil, U. Schelese, E. Roeckner, *Science* **239**, 504 (1988).
- M. Stuiver, P. Grootes, T. F. Braziunas, *Quat. Res.* **44**, 341 (1995).
- W. Dansgaard *et al.*, *Nature* **364**, 218 (1993).
- E. Bard *et al.*, *ibid.* **328**, 791 (1987).
- R. G. Fairbanks, *ibid.* **342**, 637 (1989).
- The SU81-18 core has been extensively radiocarbon-dated, and is presented here using the calibration method of M. Stuiver and P. J. Reimer [*Radiocarbon* **35**, 215 (1993)], method A, based on the Barbados coral U/Th- $^{14}\text{C}$  chronology (42). The time-depth curve was a best-fit fourth-order polynomial to all calibrated dates available (38). We recognize that the pre-Holocene  $^{14}\text{C}$ -calibration issue is not resolved (42), such that the temporal relationships between  $^{14}\text{C}$ -dated ocean cores and layer-counted ice cores cannot yet be determined with certainty. However, the recent barrier reef drillings in Tahiti (42), which demonstrate reproducibility of the U/Th chronology to at least 13.7 ka, do suggest that the isotopic maximum at 3.30 m in SU81-18 (17.5  $^{14}\text{C}$  cal ka) predates the Oldest Dryas (14.8 to 15.2 ka) event in Greenland ice cores by at least several thousand years.
- K. A. Hughen, J. T. Overpeck, L. C. Peterson, S. Trumbore, *Nature* **380**, 51 (1996).
- E. Bard, B. Hamelin, R. G. Fairbanks, A. Zindler, *ibid.* **345**, 405 (1990); B. Wohlfarth, S. Björck, G. Possnert, *Radiocarbon* **37** (no. 2), 347 (1995); E. Bard *et al.*, *Nature* **382**, 241 (1996).
- This comparison indicates that the maximum glacial stage recorded at subtropical latitudes predates the rapid warming in central Greenland (36) and the north Atlantic poleward of 50°N [H. Haffidason, H. P. Sejrup, D. K. Kristensen, S. Johnsen, *Geology* **23** (no. 12), 1059 (1995); S. J. Lehman and L. D. Keigwin, *Nature* **356**, 757 (1992)] by roughly 3 ka [T. Sowers and M. Bender, *Science* **269**, 210 (1995)]. Some confusion results from the similarity of the respective series of three intermediate deglacial stages at each latitude that are apparently not coincident in time. We therefore suggest that the Allerød/Bolling warm period was only the last of three similar progressive warming stages during the deglaciation at tropical and subtropical latitudes. Furthermore, the two intermediate cold periods (the Older Dryas and the Intra-Allerød Cold Period) that are responsible for the three-stage termination (1a) phase in Greenland and the North Atlantic, are not dominant events at lower latitudes. These appear to be absent (perhaps by smoothing) in the Huascarán record, whereas several high-frequency fluctuations are present in the zone from 149 to 155 m in Guliya, such that various correlation scenarios are possible.
- J. Kutzbach, G. Bonan, J. Foley, S. P. Harrison, *Nature* **384**, 623 (1996).
- J.-Q. Fang, *Quat. Res.* **36**, 47 (1991).
- F. M. Gasse *et al.*, *Nature* **353**, 742 (1991).
- L. D. Keigwin and G. A. Jones, *Deep-Sea Res.* **36** (no. 6), 845 (1989); L. D. Keigwin, G. A. Jones, S. J. Lehman, *J. Geophys. Res.* **96** (no. C9), 16,811 (1991); L. D. Keigwin and G. A. Jones, *ibid.* **99** (no. C6), 12,397 (1994).
- F. J. Jorissen *et al.*, *Mar. Micropaleontol.* **21**, 169 (1993); K. A. F. Zonneveld, *Palaeogeogr. Palaeoclimatol. Palaeoecol.* **122**, 89 (1996).
- We thank the many scientists, engineers, technicians and graduate students from the Byrd Polar Research Center and the Lanzhou Institute of Glaciology and Geocryology (China). Special thanks are extended to B. Koci, lead ice core driller; and to V. Mikhalenko, B. Barber, and W. Tamayo Alegre for field assistance. This work was supported by NSF's Office of Climate Dynamics and the Division of Polar Programs (grants ATM-8519794, ATM-89116635, and DPP-9014931), the National Geographic Society (grants 3323-86, 4309-90, and 4522-91), Ohio State University, and the State Committee of Science and Technology and the National Natural Science Foundation of China. This is contribution 1051 of the Byrd Polar Research Center.

7 April 1997; accepted 28 May 1997